THE JOURNAL OF BIOLOGICAL CHEMISTRY VOL. 283, NO. 18, pp. 12538–12545, May 2, 2008
Printed in the U.S.A.

Mouse EP3 α, β, and γ Receptor Variants Reduce Tumor Cell Proliferation and Tumorigenesis *in Vivo*[*]

Received for publication, January 4, 2008, and in revised form, January 23, 2008 Published, JBC Papers in Press, January 29, 2008, DOI 10.1074/jbc.M800105200

Ines M. Macias-Perez[‡§], Roy Zent[‡§¶‖], Monica Carmosino[‡], Matthew D. Breyer[‡], Richard M. Breyer[‡], and Ambra Pozzi[‡§‖1]

From the Departments of [‡]Medicine (Division of Nephrology), [§]Cancer Biology, and [¶]Cell and Developmental Biology, Vanderbilt University, Nashville, Tennessee 37232 and the [‖]Department of Medicine, Veterans Affairs Hospitals, Nashville, Tennessee 37232

Prostaglandin E_2, which exerts its functions by binding to four G protein-coupled receptors (EP1–4), is implicated in tumorigenesis. Among the four E-prostanoid (EP) receptors, EP3 is unique in that it exists as alternatively spliced variants, characterized by differences in the cytoplasmic C-terminal tail. Although three EP3 variants, α, β, and γ, have been described in mice, their functional significance in regulating tumorigenesis is unknown. In this study we provide evidence that expressing murine EP3 α, β, and γ receptor variants in tumor cells reduces to the same degree their tumorigenic potential *in vivo*. In addition, activation of each of the three mEP3 variants induces enhanced cell-cell contact and reduces cell proliferation *in vitro* in a Rho-dependent manner. Finally, we demonstrate that EP3-mediated RhoA activation requires the engagement of the heterotrimeric G protein G_{12}. Thus, our study provides strong evidence that selective activation of each of the three variants of the EP3 receptor suppresses tumor cell function by activating a G_{12}-RhoA pathway.

Colorectal cancer is the second most frequent cause of cancer-related death in the western world. An estimated 153,760 cases will be diagnosed and 52,180 people will die from this disease in the United States in 2007 (1). Overexpression of cyclooxygenase-2 (2–5) and subsequent prostaglandin production (6, 7) have been widely documented in colorectal cancer, and epidemiologic studies have shown that nonsteroidal anti-inflammatory drugs reduce the incidence of colorectal cancer mortality by decreasing the formation of PGE_2,[2] the primary prostaglandin generated in colorectal tumors (8, 9).

PGE_2 exhibits a broad range of biological actions in diverse tissues by binding to its four distinct G protein-coupled receptor subtypes designated EP1, EP2, EP3, and EP4 (10). The EP1 receptor induces mobilization of intracellular calcium; the EP2 and EP4 receptors couple to stimulatory G proteins (G_s) and signal by increasing intracellular cAMP level, whereas the EP3 receptor couples to an inhibitory G protein (G_i) and reduces cAMP synthesis (11). In the mouse, alternative splicing generates three EP3 variants, α, β, and γ, which contain carboxyl tails of 30, 26, and 29 amino acids that do not share any structural motifs or hydrophobic features. The amino acid sequence of the tails is thought to modulate signal transduction. In this context, EP3α and EP3β couple to G_i and inhibit adenylate cyclase (12, 13), whereas the EP3γ couples to G_s, in addition to G_i, and evokes cAMP production (13). Moreover, EP3 has been demonstrated to activate the small GTPase Rho in various cell types, resulting in stress fiber formation and neurite retraction (14–16).

At present, little is known on the contribution of the EP3 splice variants to tumor cell function. Unlike the other EP receptors, EP3 expression is decreased in colon cancer in mice, rats, and humans when compared with normal mucosa (17). Similar results were found in mammary tumors, suggesting that EP3 down-regulation might be a general feature of tumors (18). In a carcinogen-induced mouse model of colorectal cancer, increased colon carcinoma was found in EP3-null mice; however, deletion of the EP3 receptor did not alter the early stage of colon cancer, namely aberrant crypt formation, suggesting that EP3 impacts later stages of colon cancer progression (17). Furthermore, only one of eleven human colon cancer cell lines screened for EP receptor expression expressed EP3, and when that cell line was treated with an EP3 agonist its viability decreased by 30% (17). Taken together, these results suggest that EP3 expression confers a growth disadvantage to colon cancer cells, and it may play a protective role against colon cancer progression.

Because little is known about the mechanisms whereby EP3 decreases tumorigenesis, we expressed murine EP3 α, β, and γ receptor variants in tumor cells and determined their role both *in vivo* and *in vitro*. We provide evidence that overexpression of each of the three variants reduces *in vivo* tumorigenic potential to the same degree. Similarly, selective activation of each of the three murine EP3 receptor variants *in vitro* induces increased cell-cell contact and decreases cell proliferation. These effects were mediated by G_{12}-dependent activation of RhoA. Thus, selective activation of each of the three EP3 receptor variants decreases tumorigenic potential by activating a G_{12}-RhoA pathway.

* This work was supported by National Institutes of Health Grants RO1-CA94849 (to A. P.), RO1-DK074359 (to A. P.), and RO1-DK69921 (to R. Z.), by a merit award from the Department of Veterans Affairs (to R. Z.), by National Institutes of Health Grant DK37097 (to R. M. B. and M. D. B.), and by funding from Philip Morris USA Inc. (to A. P. and R. M. B.). The costs of publication of this article were defrayed in part by the payment of page charges. This article must therefore be hereby marked "*advertisement*" in accordance with 18 U.S.C. Section 1734 solely to indicate this fact.

[1] To whom correspondence should be addressed: Dept. of Medicine, Division of Nephrology, Medical Center North, B3109, Vanderbilt University, Nashville, TN 37232. Tel.: 615-322-4637; Fax: 615-322-4690; E-mail: ambra.pozzi@vanderbilt.edu.

[2] The abbreviations used are: PGE_2, prostaglandin E_2; EP, E-prostanoid receptor; MAPK, mitogen-activated protein kinase; mEP3, mouse EP3; ERK, extracellular signal-regulated kinase.

EXPERIMENTAL PROCEDURES

Reagents—Prostaglandins were purchased from Cayman Chemicals (Ann Arbor, MI). M&B28767 was a generous gift from Dr. M. Caton (Rhone Poulanc Pharmaceuticals), the plasmid of constitutively activated RhoA (G14V) was a gift from Dr. Brent Polk (Vanderbilt University), and the expression plasmid for *Clostridium botulinum* C3 toxin was a gift from Dr. Richard Neubig (University of Michigan). The expression plasmids of constitutively activated and dominant negative G protein subunits α_i, α_{12}, and α_{13} were purchased from UMR cDNA Resource Center (University of Missouri, Rolla, MO). [^{3}H]PGE$_2$ was purchased from Amersham Biosciences. Pertussis toxin, BAPTA/AM, PD 98059, Y-27632, and wortmannin were purchased from Calbiochem (La Jolla, CA). Fetal bovine serum and Dulbecco's modified Eagle's medium were obtained from Hyclone (Logan, UT). Penicillin/streptomycin, L-glutamine, and G418 was purchased from Invitrogen. Effectene transfection reagent was purchased from Qiagen.

Expression of mEP3 Variants in HEK293 and HCT116 Cells—The mouse EP3 (mEP3) α, β, and γ variants were subcloned into pcDNA3 using EcoRI and XhoI restriction sites, and a Myc tag was added at the extracellular N terminus. HEK293 and HCT116 cells were stably transfected with each pcDNA3/mEP3 variant or pcDNA3 empty vector using Effectene transfection reagent. The cells were selected by the addition of G418, and cell populations expressing equal levels of each mEP3 variant were sorted by flow cytometry.

Flow Cytometry—Empty vector-transfected or mEP3-expressing cells were incubated with anti-Myc antibody (9E10, sc-40; Santa Cruz, CA) followed by phycoerythrin-conjugated anti-mouse secondary antibody (Jackson Immunoresearch, West Grove, PA). Polyclonal cell populations expressing equal levels of the various mutants were selected by flow cytometry.

Radioligand Binding Assay—Empty vector-expressing or mEP3-expressing HEK293 cells were lysed in lysis buffer (15 mM HEPES, pH 7.6, 5 mM EDTA, 5 mM EGTA, and 2 mM phenylmethylsulfonyl fluoride), after which membrane-rich fractions were prepared as previously described (19). One-point binding experiments were performed with 50 μg of membrane preparation incubated in the presence of 2 nM of [^{3}H]PGE$_2$ with or without 5 μM sulprostone, as described (19). For saturation binding experiments, 5 μg of membranes were incubated with [^{3}H]PGE$_2$ at the indicated concentrations in the absence (total binding) or presence (nonspecific binding) of 10 μM PGE$_2$. The expression level (B_{max}) and [^{3}H]PGE$_2$ binding affinities (K_d) of EP3-expressing cells were determined using a one-site binding model (Prism) and are shown as the means ± S.E. of triplicate samples. Three independent experiments were performed in triplicate.

Intracellular Ca^{2+} Assay—Mobilization of intracellular calcium was measured on a FLEXstation system (Molecular Devices, Sunnyvale, CA) using the FLEXstation calcium assay kit according to the manufacturer's instructions. Briefly, 50,000 cells were plated in 96-well plates. Twenty four hours later, the cells were labeled with calcium assay reagent. Some cells were treated with various concentrations of M&B28767. Fluorescence was monitored (λ_{ex} = 485 nm, λ_{em} = 525 nm), and the experiment was terminated by the addition of 10 μM ionomycin to determine maximum Ca^{2+} response. Three independent experiments were performed in quadruplicate.

Immunofluorescence—To visualize actin and ZO-1, 2×10^5 cells were plated into eight-chamber slides (Falcon; Becton Dickinson, Heidelberg, Germany) and cultured for 48 h. The cells were subsequently treated with 0.1 μM PGE$_2$, sulprostone, M&B28767, butaprost, or vehicle (Ethanol) for 4 h. The cells were fixed with 4% formaldehyde, permeabilized, and incubated with either rabbit anti-ZO-1 antibody (Zymed Laboratories) or rhodamine-phalloidin (Molecular Probes, Eugene, OR). A fluorescein-conjugated anti-rabbit secondary antibody was utilized to visualize the ZO-1 antibody. The cells were analyzed using an epifluorescence microscope (Nikon). To visualize the Myc-EP3 variants, 8-μm frozen tumor sections were incubated with mouse anti-Myc antibody (Santa Cruz; 1:100 dilution in 3% bovine serum albumin/PBS) followed by an anti-mouse secondary antibody.

Rho GTP Pulldown Assay—Equal numbers of serum-starved cells were treated with 0.1 μM M&B28767 or vehicle for 15 min, after which the levels of GTP-Rho were analyzed using the Rho pulldown kit as described by the manufacturer (Upstate Biotechnology, Lake Placid, NY). Equal volumes of total cell lysates were used to detect total levels of Rho.

Western Blot Analysis—To evaluate the effects of mEP3 activation on ERK, p38, and Akt phosphorylation, semi-confluent cells were serum-starved for 24 h and then treated with 0.1 μM M&B28767 or vehicle for 15 min. The cells were lysed, and an equal amount of cell lysates (30 μg/lane) were resolved by SDS/PAGE and transferred to Immobilon-P membranes. The membranes were immunoblotted with the phospho-antibodies designated. Equal loading was verified by stripping the membranes with β-mercaptoethanol for 1 h at 55 °C and reprobing with antibodies to total ERK, p38, or Akt antibody. All of the antibodies were obtained from Cell Signaling Technology.

To confirm overexpression of constitutively active or dominant negative Rho and/or selective G protein α subunits, 50 μg of total cell lysates from untransfected or 48 h transfected cells were analyzed by Western blot analysis using rabbit anti-Rho, anti-Gα_{i2} (T-19), anti-Gα_{12} (S-20), or anti-Gα_{13} (A-20). Equal loading was verified by probing with rabbit anti-FAK (C-20). All of the antibodies were from obtained from Santa Cruz.

Cell Proliferation—Cell proliferation was evaluated as previously described (20). Briefly, 5×10^3 cells were plated into 96-well plate in the presence of 2.5% fetal calf serum. Twenty-four hours later, the cells were pulsed with [^{3}H]thymidine (1 μCi/well) with or without 0.1 μM PGE$_2$, M&B28767, sulprostone, or butaprost. For Rho inhibitor studies, 10 μM of Y-27632 were added to appropriate wells. Forty-eight h later, the cells were lysed with 2% SDS and counted with a β-counter. Four independent experiments were performed in quadruplicate.

Tumor Growth in Nude Mice—Athymic nude mice were injected subcutaneously with 1×10^6 cells and euthanized 35 days post-injection. The mice were anesthetized and euthanized by Institutional Animal Care and Use Committee approved procedures. The tumors were harvested, measured, and embedded in OCT for frozen sections. The volume was

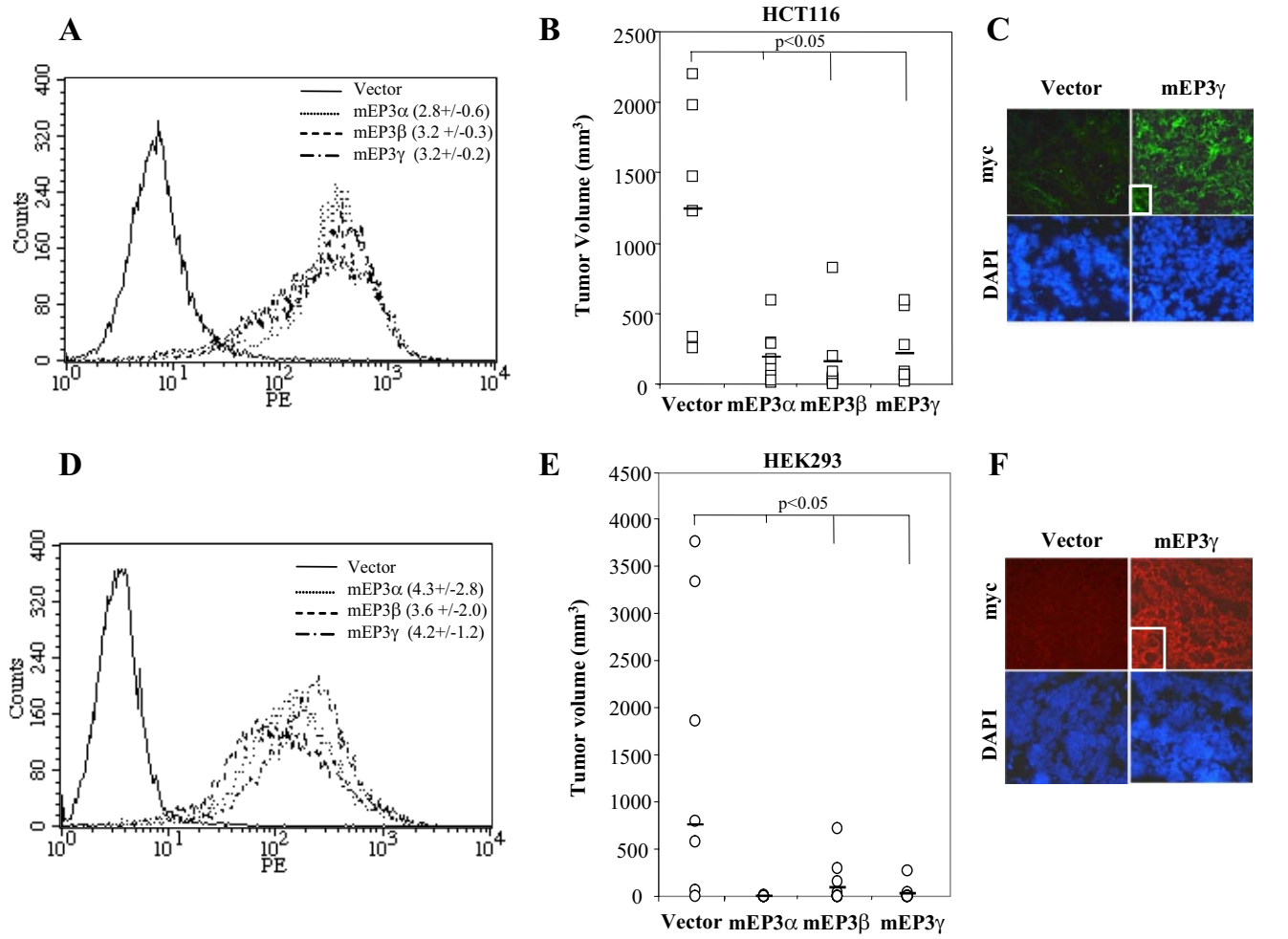

FIGURE 1. **The mEP3 receptor variants inhibit growth *in vivo*.** *A*, flow cytometry of stably transfected HCT116 cells with mEP3 receptor variants labeled with anti-Myc antibody. mEP3 receptor expression is displayed by a shift in mean fluorescent intensity compared with empty vector-transfected HCT116 cells. The values represent the means ± S.D. of mean fluorescent intensity of three independent experiments. *B*, 1×10^6 empty vector-transfected and mEP3-expressing HCT116 cells were injected subcutaneously into nude mice ($n = 10$/cell type). 35 days later the mice were sacrificed, and tumor volume was evaluated as described under "Experimental Procedures." The *open squares* represent the volume of single tumors, whereas the *bars* represent the means. *C*, frozen sections of tumors derived from the tumors indicated (only mEP3γ shown) were stained with anti-Myc antibody to confirm the *in vivo* expression of the mEP3 receptor variants. *D*, flow cytometric analysis of stably transfected HEK293 cells with mEP3 receptor variants was performed as described in *A*. *E*, 1×10^6 empty vector-transfected and mEP3-expressing HEK293 cells were injected subcutaneously into nude mice ($n = 10$/cell type). 35 days later mice were sacrificed, and tumor volume was evaluated as described under "Experimental Procedures." The *open circles* represent the volume of single tumors, whereas the *bars* represent the mean. *F*, frozen sections of the tumors indicated (only mEP3γ shown) were stained with anti-Myc antibody to confirm the *in vivo* expression of the mEP3 receptor variants. *DAPI*, 4′,6′-diamino-2-phenylindole.

determined according to the equation: volume = [length × width^2] × 0.5.

Statistical Analysis—The Student's *t* test was used for comparisons between two groups, and analysis of variance using Sigma-Stat software was used for statistical difference between multiple groups. $p < 0.05$ was considered statistically significant.

RESULTS

The mEP3 Receptor Variants Inhibit Tumor Cell Growth in Vivo—HCT116 colon cancer cells are known to express EP1, EP2, and EP4, but not EP3 (17). To evaluate the role of mEP3 receptor variants on tumor cell growth, HCT116 colon cancer cells were stably transfected with mouse EP3 (mEP3) α, β, and γ cDNAs Myc-tagged at the extracellular N terminus. Cell populations expressing comparable levels of the receptor variants were isolated by fluorescence-activated cell sorter using an anti-Myc antibody (Fig. 1*A*). When athymic/nude mice were injected subcutaneously with mEP3-expressing or empty vector-transfected HCT116 cells, tumors formed in nearly all the mice within 35 days post-injection; however, tumors derived from empty vector-transfected HCT116 cells were significantly larger than those derived from mEP3-expressing HCT116 cells (Fig. 1*B*). All of the tumors derived from mEP3-expressing HCT116 cells exhibited positive staining for Myc, indicating that mEP3 receptor expression was maintained during tumor formation (Fig. 1*C*, only mEP3γ shown).

To further confirm the suppressive role of the mEP3 receptor variants in tumor cell growth, we stably expressed the mEP3 receptor variants in HEK293 cells, because they are tumorigenic *in vivo* (21) and are commonly utilized to study prostanoid receptor signaling (22–26). As with the HCT116 cells, HEK293 cells were sorted for comparable cell surface expression of the mEP3 receptor variants by flow cytometry (Fig. 1*D*).

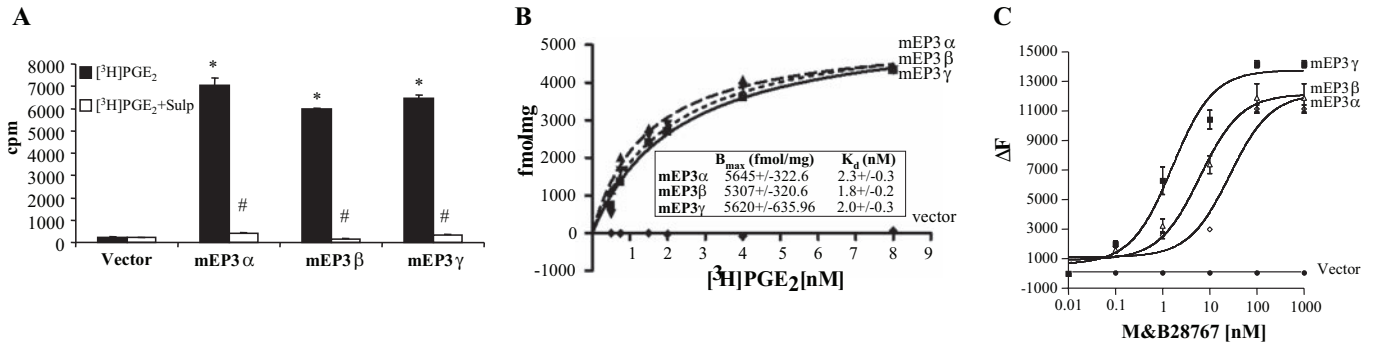

FIGURE 2. **Characterization of the mEP3 receptor variants.** *A*, one-point ligand binding assay on 50-μg membranes from empty vector-transfected and mEP3-expressing HEK293. The *bars* and *error bars* are the means ± S.D. of triplicate samples. *, significant differences ($p < 0.05$) between vehicle-treated and PGE_2-treated membranes; #, significant differences ($p < 0.05$) between PGE_2-treated and PGE_2+Sulprostone-treated membranes. *B*, saturation isotherm analysis of [^{3}H]PGE_2 binding to empty vector-transfected and mEP3-expressing HEK293 cells. The membranes (5 μg) were incubated with [^{3}H]PGE_2 at the concentrations indicated in the absence (total binding) or presence (nonspecific binding) of 10 μM PGE_2, as described under "Experimental Procedures." Specific binding (total-nonspecific) is shown. The values in the *inset* represent the means ± S.D. of one representative experiment performed in triplicate. *C*, dose response of M&B28767-induced intracellular calcium mobilization was evaluated in empty vector-transfected and mEP3-expressing HEK293 cells as described under "Experimental Procedures."

When these cells were injected into athymic/nude mice, empty vector-transfected HEK293 cells formed tumors more readily and larger than mEP3-expressing HEK293 cells (Fig. 1*E*). In addition, all of the tumors from mEP3-expressing HEK293 cells exhibited positive staining for Myc, indicating that these cells maintained EP3 expression during tumor formation (Fig. 1*F*, mEP3γ shown). Therefore, expression of the mEP3 receptor variants by either HCT116 colon cancer or HEK293 cells results in decreased tumor growth *in vivo*.

Characterization of mEP3 Receptor Variants in HEK293 Cells—HEK293 cells were used for all of the *in vitro* assays described below as (i) the *in vivo* growth inhibitory effect of mEP3-expressing expressing HEK293 cells was similar to that of mEP3-expressing HCT116 cells (Fig. 1); (ii) HEK293 cells express little endogenous EP receptors and are routinely used to study exogenously expressed prostanoid receptors (22–26); and (iii) unlike mEP3-expressing HCT116 cells, HEK293 cells maintain robust expression of the mEP3 variants over multiple passages.

To confirm native ligand binding to the mEP3 variants, equal amounts of cell membranes were labeled with radioactive PGE_2 in the absence or presence of saturating levels of the selective EP3 agonist sulprostone (Fig. 2*A*). Binding to the EP3 variants was similar and equally inhibited by cold sulprostone. In contrast, empty vector-transfected cells exhibited no specific PGE_2 binding activity. To confirm comparable receptor number, a saturation isotherm binding assay was performed. As shown in Fig. 2*B*, [^{3}H]PGE_2 binding affinities (K_d) and expression levels (B_{max}) were comparable among each of the three mEP3 receptor variant-expressing cells, whereas no binding was observed with membranes derived from empty vector-transfected cells.

Because activation of the mEP3 receptor variants leads to increased intracellular calcium (27), the ability of the two selective EP3 agonists M&B28767 (Fig. 2*C*) and sulprostone (not shown) to induce intracellular calcium mobilization was determined. Each of the three mEP3 variants mobilized calcium in a concentration-dependent manner after stimulation with EP3 agonists (Fig. 2*C*). In contrast, no calcium mobilization was detected in empty vector-transfected cells. Thus, each of the three mEP3 receptor variants was functionally expressed in HEK293 cells.

mEP3 Receptor Variants Promote Cell Clustering and Inhibit Cell Growth in Vitro—To determine the biological effects of mEP3-expressing HEK293 cells, their morphology was examined upon treatment with M&B28767 (Fig. 3*A*). Cells expressing each of the three mEP3 variants formed clusters within 4 h of receptor activation, whereas empty vector-expressing HEK293 cells remained scattered and had a more mesenchymal phenotype (Fig. 3*A*). The cell clustering was associated with increased cell-cell contact, as shown by membrane localization of ZO-1, a marker for tight junctions (Fig. 3*A*). Immunoblots for ZO-1 showed no change in ZO-1 expression (not shown), indicating that the EP3-mediated cell-cell contact is due primarily to an increase in ZO-1 membrane localization.

To confirm receptor selectivity of this phenomenon, mEP3-expressing HEK293 cells were exposed to the native EP ligand PGE_2, the EP3 selective agonist sulprostone, or the EP2 selective agonist butaprost (Fig. 3*B*). As with M&B28767, all three mEP3 variants caused HEK293 cells to cluster and display enhanced cell-cell contact when stimulated with PGE_2 or sulprostone but not with butaprost. Because this morphological change was not reversed when medium of M&B28767-stimulated cells was replaced with normal media (Fig. 3*C*), we concluded that EP3 activation has a lasting effect on cell morphology.

We next determined whether activation of the mEP3 variants in HEK293 cells led to decreased cell growth *in vitro*, thus paralleling the *in vivo* reduction in tumor volume. As shown in Fig. 3*D*, mEP3-expressing HEK293 cells exhibit a 30–40% reduction in growth when treated with PGE_2, M&B28767, or sulprostone compared with empty vector-expressing HEK293 cells. As expected, the EP2 selective agonist butaprost had no effect on cell growth. Collectively, these data suggest that all three mEP3 variants induce cell clusters with enhanced cell-cell contact as well as decreased cell growth *in vitro*.

The mEP3 Receptor Variants Activate ERK and RhoA—To characterize the intracellular signaling pathways activated by the mEP3 receptor variants, the phosphatidylinositol 3-kinase

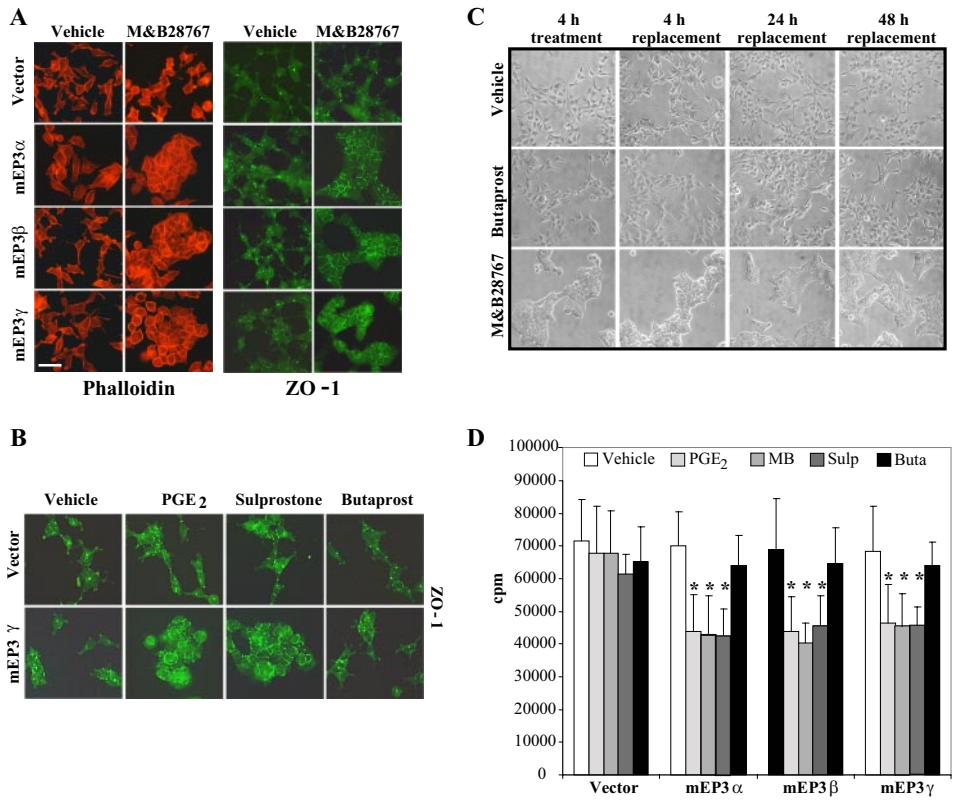

FIGURE 3. **Activation of the mEP3 receptor variants enhances cell-cell contact and reduces growth *in vitro*.** *A*, empty vector-transfected and mEP3-expressing HEK293 cells were treated with vehicle or 0.1 μM M&B28767. After 4 h, the cells were stained with rhodamine-phalloidin and anti-ZO-1 antibody to visualize the cytoskeleton and tight junctions, respectively. *Scale bar*, 20 μm. The images are representative of three independent experiments. *B*, empty vector-transfected and mEP3-expressing HEK293 cells (mEP3γ shown only) were treated with vehicle or 0.1 μM PGE_2, sulprostone, or butaprost. After 4 h the cells were stained with anti-ZO1 antibody to visualize tight junctions. *Scale bar*, 20 μm. The images are representative of three independent experiments. *C*, the cells indicated were treated with 0.1 μM M&B28767, butaprost or vehicle. After 4 h the medium was replaced with medium lacking prostanoid, and the cells were imaged 4, 24, and 48 h after medium replacement. The images shown are representative of three independent experiments. *D*, [^{3}H]thymidine incorporation on empty vector-transfected and mEP3-expressing HEK293 cells treated with vehicle, PGE_2, M&B28767 (*MB*), sulprostone (*Sulp*), or butaprost (*Buta*) was evaluated as described under "Experimental Procedures." The *bars* and *error bars* represent the means $\pm$ S.D. of one experiments performed in quadruplicate. *, significant differences ($p < 0.05$) between vehicle-treated and prostanoid-treated cells.

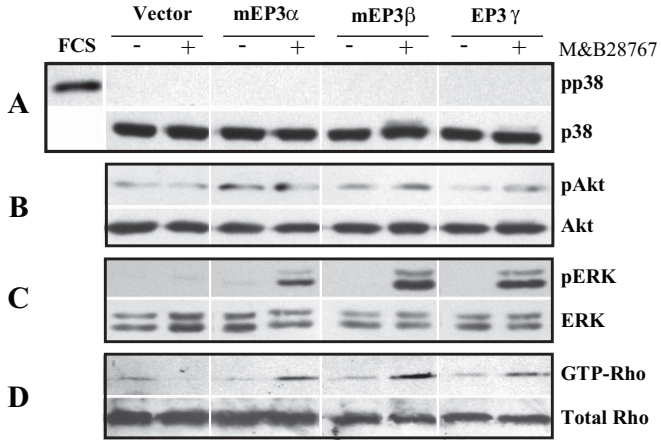

FIGURE 4. **The mEP3 receptor variants activate ERK and Rho.** *A–C*, serum-starved cells were treated with vehicle or 0.1 μM M&B28767 for 15 min, and the levels of phosphorylated p38 MAPK, Akt, and ERK as well as total p38 MAPK, Akt, and ERK were analyzed by Western blot in 30 μg of total cell lysates. *FCS* represents serum cells stimulated for 15 min with 10% fetal calf serum as positive control. *D*, Rho pulldown assay performed on cells lysates of serum-starved cells treated with vehicle or 0.1 μM M&B28767 for 15 min. Bound GTP-Rho was detected by immunoblotting with anti-Rho antibody (*top*). The total cell lysates were used to detect the levels of total Rho (*bottom*).

and MAPK pathways were examined, because PGE_2 has been reported to activate both pathways (20, 28–31). Whereas treatment with M&B28767 did not result in p38 MAPK or Akt activation (Fig. 4, *A* and *B*), ERK activation was evident in all three mEP3-expressing cells within 15 min of receptor activation (Fig. 4*C*). Because the mEP3 receptor variants have been shown to induce Rho activation in PC-12 and Madin-Darby canine kidney cells (14–16), we also evaluated the effect of mEP3 activation on Rho GTPases. Treatment with M&B28767 led to a 3–4-fold increase in RhoA activation by cells expressing each of the three mEP3 splice variants as compared with empty vector-transfected HEK293 cells (Fig. 4*D*). Thus, activation of the EP3 receptor leads to ERK and RhoA activation in HEK293 cells.

RhoA Mediates the mEP3-induced Morphological Change and Growth Inhibition—To explore the mechanism(s) by which mEP3 variants promoted cell-cell contact, we made use of selective pharmacological inhibitors. Forskolin (not shown) and isobutylmethylxanthine (Fig. 5*A*), which elevate cAMP levels; the cAMP-dependent protein kinase inhibitor H-89 (not shown); the protein kinase C inhibitor Bisindolylmaleimide (not shown), BAPTA/AM, a calcium chelator (Fig. 5*A*); the MAPK/ERK kinase inhibitor PD98059 (Fig. 5*A*) and the phosphatidylinositol 3-kinase inhibitor wortmannin (Fig. 5*A*) were not able to block EP3-mediated morphological change (Fig. 5*A*). In contrast, the Rho kinase inhibitor Y-27632 and expression of the C3 *C. botulinum* toxin, which inactivates Rho, blocked the EP3-induced morphological change in all three variant-expressing cells (Fig. 5*A*, mEP3γ-expressing cells shown only). Expression and activity of the C3 toxin was confirmed by comparing RhoA activation after M&B28767 treatment in mEP3-expressing HEK293 cells with or without C3 transfection (Fig. 5*B*, mEP3γ expressing cells shown only).

To determine whether Rho was also involved in the EP3-mediated cell growth inhibition, the effect of the Rho kinase inhibitor Y-27632 on cell proliferation was determined. As shown in Fig. 5*C*, treatment with Y-27632 reversed both PGE_2- and M&B28767-mediated cell growth inhibition, and this effect was independent of the mEP3 variant expressed. These results suggest that the EP3-induced morphological change and reduction in cell growth are both mediated by Rho.

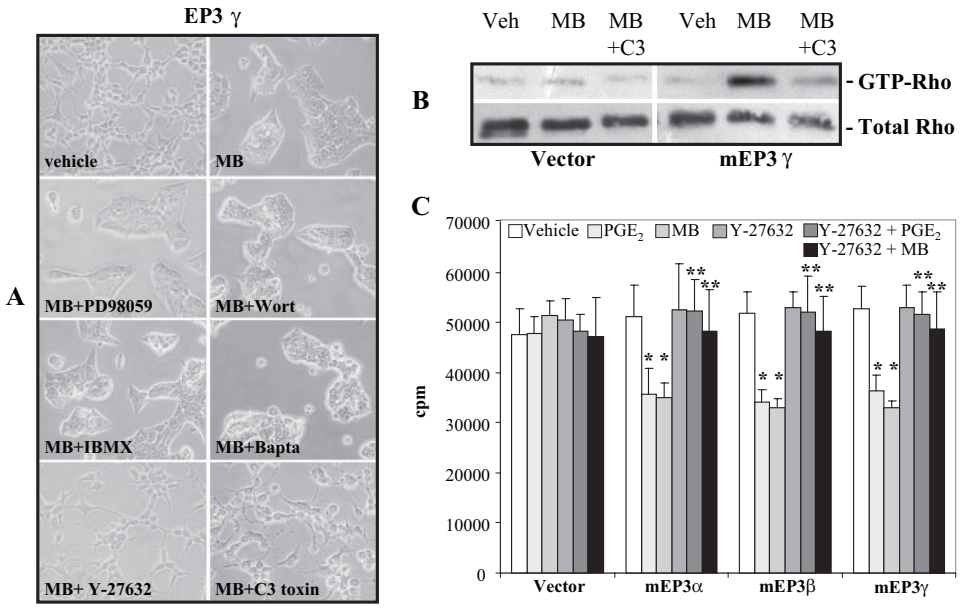

FIGURE 5. **mEP3-induced morphological change and growth inhibition are mediated by Rho.** *A*, mEP3-expressing HEK293 cells (mEP3γ shown only) were serum-starved for 12 h in the presence or absence of PD-98059 (5 μM), wortmannin (*Wort*, 100 nM), isobutylmethylxanthine (*IBMX*, 0.5 mM), 5 μM BAPTA/AM (5 μM), or Y-27632 (5 μM) or transfected for 48 h with the C3 toxin expression plasmid. The cells were subsequently treated with vehicle (*Veh*) or 0.1 μM M&B28767 (*MB*), and their morphology was evaluated 4 h after treatment. The images are representative of three independent experiments. *B*, Rho pulldown assay was performed on cells lysates of serum-starved empty vector-transfected and mEP3-expressing HEK293 (mEP3γ shown only) cells treated as indicated. GTP-Rho was detected by immunoblotting with anti-Rho antibody (*top*). Total cell lysates were used to detect the levels of total Rho (*bottom*). *C*, [^{3}H]thymidine incorporation assay on empty vector-transfected and mEP3-expressing HEK293 cells incubated in the presence or absence of 10 μM Y-27632, 0.1 μM PGE_2, and 0.1 μM M&B28767 (*MB*) was evaluated as described under "Experimental Procedures." The *bars* and *error bars* represent the means ± S.D. of a representative experiment performed in quadruplicates. *, significant differences ($p < 0.05$) between vehicle and PGE_2- or MB-treated cells. **, significant differences ($p < 0.05$) between MB- and MB+Y-27632 or PGE_2- and PGE_2+Y-27632 treated cells.

mEP3 Receptor Regulates Cell Morphology via G_{12}—Although the EP3 receptor variants are coupled to adenylate cyclase, inhibition through G_i via pertussis toxin did not suppress the morphological change induced by EP3 agonists (data not shown), suggesting that this action is not mediated by G_i. Forskolin (not shown) or isobutylmethylxanthine (Fig. 5*A*) also failed to block the EP3-induced morphological change, suggesting that this action is not mediated by G_s either. To determine whether activation of RhoA was sufficient to induce the morphological changes seen in the mEP3-expressing HEK293 cells, we expressed a dominant active Rho (G14V) into empty vector-transfected or mEP3γ-expressing HEK293 cells (Fig. 6*A*). As shown in Fig. 6*B*, dominant active Rho was sufficient to induce cell clustering in both cell types, suggesting that RhoA is downstream of the EP3 receptor.

Because several reports have shown that constitutively activated $G\alpha_{12}$ and $G\alpha_{13}$ can stimulate Rho-dependent stress fiber formation and focal adhesion assembly (14–16), we determined whether the EP3-mediated cell clustering was via $G\alpha_{12}$ and/or $G\alpha_{13}$. To do so, EP3γ-expressing HEK293 cells were transfected with constitutively activated G_i (negative control), $G\alpha_{12}$, and $G\alpha_{13}$ (Fig. 6*C*). Only constitutively activated $G\alpha_{12}$ and $G\alpha_{13}$ induced base-line morphological changes in all the transfected cells, suggesting that both $G\alpha_{12}$ and $G\alpha_{13}$ can mediate the Rho-induced morphological cell change. Similar results were obtained with mEP3α- and mEP3β-expressing HEK293 cells (not shown).

To determine which of the two G proteins transduces the EP3-mediated Rho activation, EP3γ-expressing HEK293 cells were transfected with dominant negative G_i, $G\alpha_{12}$, and $G\alpha_{13}$ (Fig. 7*A*) and subsequently treated with M&B28767 for 4 h. As shown in Fig. 7*B*, dominant negative $G\alpha_{12}$, but not dominant negative G_i or $G\alpha_{13}$, prevented the EP3-induced cells from clustering and from developing an epithelial-like morphology. Similar results were obtained with mEP3α- and mEP3β-expressing HEK293 cells (not shown). These results indicate that the mEP3 receptor variants induce cell clustering and increase cell-cell contact via a G_{12}-Rho pathway.

DISCUSSION

Unlike EP1, EP2, and EP4 receptors, it has been shown that deletion of the EP3 receptor accelerates late stages of tumor progression (17). In this study, we provide the novel evidence that overexpression of the α, β, and γ mouse EP3 receptor variants in tumor cells reduces their tumorigenic potential *in vivo*. In addition, activation of these mEP3 variants causes enhanced cell-cell contact and reduces cell growth *in vitro* through Rho activation. Finally, we demonstrate that EP3-mediated Rho activation requires the engagement of the heterotrimeric G protein G_{12}, but not G_{13}. Based on these results we propose that activating EP3 might be a strategy to decrease tumorigenesis *in vivo*.

Our *in vivo* findings demonstrate that overexpression of mEP3 variants decreases the tumorigenic potential of two different tumor cell lines. These observations support the finding that mice lacking EP3 develop an increased incidence of azoxymethane-induced colon carcinoma, despite the fact that no difference in the incidence and development of aberrant crypt foci, putative precursors of colon cancer, were observed between wild type and EP3-null mice (17). Furthermore, our data agree with the findings that EP3 mRNA expression is decreased in mammary and colon tumors compared with normal mucosa (17, 18) and that EP3 expression was absent in ten of eleven human colon cancer cell lines screened (17). Taken together these data suggests that EP3 expression and activation plays a suppressive role in tumor development *in vivo* and that its down-regulation by tumor cells is advantageous for cancer progression.

In this study we demonstrate that there is no difference in tumor formation/growth among the tumor cells expressing either α, β, or γ mouse EP3 variants. Similarly, the degree of enhanced cell-cell contact and/or decreased cell proliferation

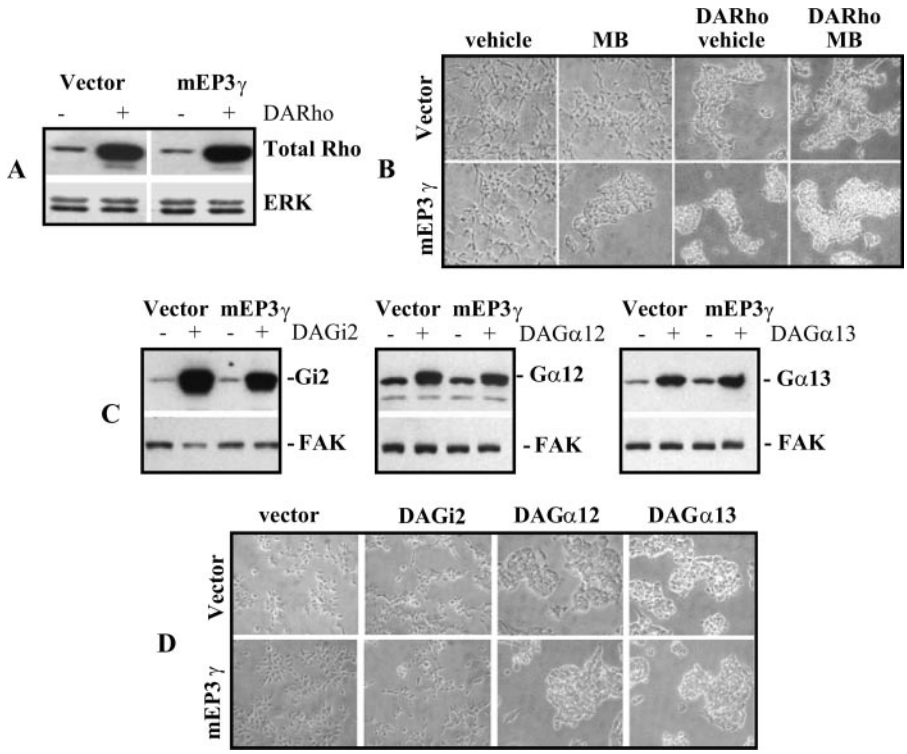

FIGURE 6. **Activated Rho, G_{12} and G_{13} induce a morphological change characterized by enhanced cell-cell contact.** *A*, the cells indicated were transfected with empty vector or dominant active Rho (*DARho*), and the levels of Rho were evaluated 48 h after transfection by Western blot analysis in 30 μg of total cell lysates. The membranes were subsequently incubated with anti-FAK antibody to verify equal loading. *B*, 48 h empty vector- or DARho-transfected cells were treated with vehicle or 0.1 μM M&B28767, and their morphology was evaluated 4 h after treatment. The images are representative of three independent experiments. *C*, the cells indicated were transfected with only or dominant active G_{i2}, $G\alpha_{12}$, or $G\alpha_{13}$, and the levels of these G protein α subunits were evaluated 48 h after transfection by Western blot analysis in 30 μg of total cell lysates. The membranes were subsequently incubated with anti-FAK antibody to verify equal loading. *D*, the cells indicated were transfected with the constructs indicated above. 48 h later cell morphology was evaluated in 4-h vehicle-treated cells. The images are representative of three independent experiments.

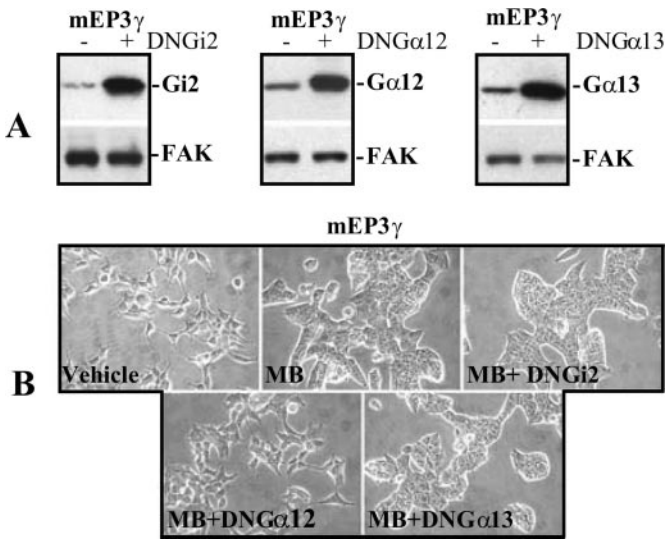

FIGURE 7. **The mEP3-induced morphological change is mediated by G_{12}.** *A*, mEP3-expressing HEK293 (mEP3γ shown only) were transfected with empty vector or dominant negative G_i, $G\alpha_{12}$, or $G\alpha_{13}$, and the levels of these G protein α subunits were evaluated 48 h after transfection by Western blot analysis in 30 μg of total cell lysates. The membranes were subsequently incubated with anti-FAK antibody to verify equal loading. *B*, mEP3-expressing HEK293 cells (mEP3γ shown only) were transfected with the constructs indicated above. Forty-eight h later the cells were either treated with vehicle or 0.1 μM M&B28767, and their morphology was evaluated 4 h after treatment. The images are representative of three independent experiments.

in vitro is comparable among the HEK293 cells expressing the three different EP3 receptor variants. Furthermore, we demonstrate that all three EP3 variants can equally activate ERK and Rho and, like others have previously shown, they promote intracellular calcium mobilization in a similar dose- and time-dependent manner (27). These results contrast with the fact that functional differences among the murine splice variants occurs with respect to (i) coupling to different signal transduction pathways (32), (ii) sensitivities to agonist-induced desensitization (33), (iii) extents of constitutive activity (34), (iv) intracellular trafficking patterns (35), (v) efficiency in calcium mobilization (Fig. 2*C*), and (vi) agonist-induced internalization patterns (36). Thus, the signaling pathways that control tumor cell growth, cell-cell contact, and tumorigenic potential are mediated by a conserved pathway activated by each of the three mouse EP3 receptor variants.

Among classical second messenger pathways, the EP3 receptor is coupled to adenylate cyclase inhibition through G_i (34, 37); however, the EP3-induced morphological changes in the HEK293 cells were not suppressed by pertussis toxin treatment, indicating that its action was mediated by a pertussis toxin-insensitive heterotrimeric G protein. The mouse EP3α and β as well as bovine EP3B receptor variants have been shown to promote stress fiber formation and neurite retraction via the via small GTPase Rho (14, 16). In addition, constitutively active G_{12} and G_{13} promote Rho activation (38), suggesting that one or both of these G proteins may signal to Rho via EP3. Despite these findings, no studies have clearly delineated which of these G proteins promotes EP3-mediate Rho activation. Our *in vitro* data provide strong evidence that G_{12}, but not G_{13}, is required for EP3 to activate Rho in HEK293 cells. In addition, we report that, like EP3α and EP3β, the mouse EP3γ variant is able to activate Rho.

Our conclusions that each of the three murine EP3 variants mediates Rho activation via G_{12} is based on the observation that overexpression of dominant negative G_{12}, but not G_{13}, prevents the EP3-induced enhanced cell-cell contact. Although dominant negative studies have some limitations, they are the best and most acceptable methods of distinguishing between G_{12}-*versus* G_{13}-mediated activity and have been used to identify G_{12} and/or G_{13} coupling for G protein-coupled receptors such the α_1-adrenoreceptor, the vasopressin V_{1a} receptor, and the serotonin receptor 2c subtype (5-HT_{2C}), to name few (39).

The most striking finding of our study is that EP3-mediated Rho activation inversely correlates with cell proliferation. This observation contrasts with others who have shown that Rho activation in many tumor types plays a positive role in tumorigenesis and metastasis by enhancing cell migration, proliferation, as well as protease synthesis and consequent matrix remodeling (40, 41). A possible explanation for our finding is that EP3-mediated Rho activation leads to increased cell-cell contact, resulting in contact inhibition and cell growth arrest. Contact inhibition is a well known mechanism of controlling cell growth and is thought to be mediated at least in part by blocking the growth factor and integrin-mediated stimuli required for cells to proliferate (42). Furthermore it has been recently shown that Rho activation is necessary to establish complete cell-cell adhesion (43). Thus, because we show that EP3 can induce long lasting cell-cell contact, it is plausible this is a major mechanism whereby this receptor decreases cell proliferation *in vitro* and tumorigenesis *in vivo*.

Although our data indicate that selective activation of EP3 in tumor cells can be viewed as a method of decreasing tumor formation, EP3 expression is down-regulated or absent in colon and mammary tumors (17, 18). The molecular mechanisms by which EP3 expression is down-regulated are currently unknown. One possible mechanism is by methylation because demethylating agents restores EP3 expression (17); however, hypermethylation of the EP3 gene has yet to be reported. Despite this, our study strongly suggests a novel anti-tumorigenic function of PGE_2 through the EP3 receptor.

Acknowledgment—We thank Cathy Alford at the Department of Veterans affairs for help with the flow cytometric analysis.

REFERENCES

1. Jemal, A., Siegel, R., Ward, E., Murray, T., Xu, J., and Thun, M. J. (2007) *CA Cancer J. Clin.* **57,** 43–66
2. Eberhart, C. E., Coffey, R. J., Radhika, A., Giardiello, F. M., Ferrenbach, S., and DuBois, R. N. (1994) *Gastroenterology* **107,** 1183–1188
3. Kargman, S. L., O'Neill, G. P., Vickers, P. J., Evans, J. F., Mancini, J. A., and Jothy, S. (1995) *Cancer Res.* **55,** 2556–2559
4. Kutchera, W., Jones, D. A., Matsunami, N., Groden, J., McIntyre, T. M., Zimmerman, G. A., White, R. L., and Prescott, S. M. (1996) *Proc. Natl. Acad. Sci. U. S. A.* **93,** 4816–4820
5. Sano, H., Kawahito, Y., Wilder, R. L., Hashiramoto, A., Mukai, S., Asai, K., Kimura, S., Kato, H., Kondo, M., and Hla, T. (1995) *Cancer Res.* **55,** 3785–3789
6. Oka, M., Inaba, A., Uchiyama, T., Hazama, S., Shimoda, K., Suzuki, M., and Suzuki, T. (1994) *Am. J. Surg.* **167,** 264–267
7. Pugh, S., and Thomas, G. A. (1994) *Gut* **35,** 675–678
8. Thun, M. J., Namboodiri, M. M., Calle, E. E., Flanders, W. D., and Heath, C. W., Jr. (1993) *Cancer Res.* **53,** 1322–1327
9. Thun, M. J., Namboodiri, M. M., and Heath, C. W., Jr. (1991) *N. Engl. J. Med.* **325,** 1593–1596
10. Boie, Y., Stocco, R., Sawyer, N., Slipetz, D. M., Ungrin, M. D., Neuschafer-Rube, F., Puschel, G. P., Metters, K. M., and Abramovitz, M. (1997) *Eur. J. Pharmacol.* **340,** 227–241
11. Hata, A. N., and Breyer, R. M. (2004) *Pharmacol. Ther.* **103,** 147–166
12. Sugimoto, Y., Negishi, M., Hayashi, Y., Namba, T., Honda, A., Watabe, A., Hirata, M., Narumiya, S., and Ichikawa, A. (1993) *J. Biol. Chem.* **268,** 2712–2718
13. Irie, A., Sugimoto, Y., Namba, T., Harazono, A., Honda, A., Watabe, A., Negishi, M., Narumiya, S., and Ichikawa, A. (1993) *Eur. J. Biochem.* **217,** 313–318
14. Hasegawa, H., Negishi, M., Katoh, H., and Ichikawa, A. (1997) *Biochem. Biophys. Res. Commun.* **234,** 631–636
15. Katoh, H., Aoki, J., Ichikawa, A., and Negishi, M. (1998) *J. Biol. Chem.* **273,** 2489–2492
16. Katoh, H., Negishi, M., and Ichikawa, A. (1996) *J. Biol. Chem.* **271,** 29780–29784
17. Shoji, Y., Takahashi, M., Kitamura, T., Watanabe, K., Kawamori, T., Maruyama, T., Sugimoto, Y., Negishi, M., Narumiya, S., Sugimura, T., and Wakabayashi, K. (2004) *Gut* **53,** 1151–1158
18. Chang, S. H., Liu, C. H., Conway, R., Han, D. K., Nithipatikom, K., Trifan, O. C., Lane, T. F., and Hla, T. (2004) *Proc. Natl. Acad. Sci. U. S. A.* **101,** 591–596
19. Breyer, R. M., Emeson, R. B., Tarng, J. L., Breyer, M. D., Davis, L. S., Abromson, R. M., and Ferrenbach, S. M. (1994) *J. Biol. Chem.* **269,** 6163–6169
20. Pozzi, A., Yan, X., Macias-Perez, I., Wei, S., Hata, A. N., Breyer, R. M., Morrow, J. D., and Capdevila, J. H. (2004) *J. Biol. Chem.* **279,** 29797–29804
21. Scherpereel, A., Gentina, T., Grigoriu, B., Senechal, S., Janin, A., Tsicopoulos, A., Plenat, F., Bechard, D., Tonnel, A. B., and Lassalle, P. (2003) *Cancer Res.* **63,** 6084–6089
22. Falcetti, E., Flavell, D. M., Staels, B., Tinker, A., Haworth, S. G., and Clapp, L. H. (2007) *Biochem. Biophys. Res. Commun.* **360,** 821–827
23. Sasaki, M., Sukegawa, J., Miyosawa, K., Yanagisawa, T., Ohkubo, S., and Nakahata, N. (2007) *Prostaglandins Other Lipid Mediat.* **83,** 237–249
24. Wilson, R. J., and Giles, H. (2005) *Br. J. Pharmacol.* **144,** 405–415
25. Hata, A. N., Lybrand, T. P., and Breyer, R. M. (2005) *J. Biol. Chem.* **280,** 32442–32451
26. Hata, A. N., Lybrand, T. P., Marnett, L. J., and Breyer, R. M. (2005) *Mol. Pharmacol.* **67,** 640–647
27. Irie, A., Segi, E., Sugimoto, Y., Ichikawa, A., and Negishi, M. (1994) *Biochem. Biophys. Res. Commun.* **204,** 303–309
28. Castellone, M. D., Teramoto, H., Williams, B. O., Druey, K. M., and Gutkind, J. S. (2005) *Science* **310,** 1504–1510
29. Kanda, N., Koike, S., and Watanabe, S. (2005) *J. Pharmacol. Exp. Ther.* **315,** 796–804
30. Kotani, M., Tanaka, I., Ogawa, Y., Suganami, T., Matsumoto, T., Muro, S., Yamamoto, Y., Sugawara, A., Yoshimasa, Y., Sagawa, N., Narumiya, S., and Nakao, K. (2000) *J. Clin. Endocrinol. Metab.* **85,** 4315–4322
31. Rao, R., Redha, R., Macias-Perez, I., Su, Y., Hao, C., Zent, R., Breyer, M. D., and Pozzi, A. (2007) *J. Biol. Chem.* **282,** 16959–16968
32. Namba, T., Sugimoto, Y., Negishi, M., Irie, A., Ushikubi, F., Kakizuka, A., Ito, S., Ichikawa, A., and Narumiya, S. (1993) *Nature* **365,** 166–170
33. Negishi, M., Sugimoto, Y., Hayashi, Y., Namba, T., Honda, A., Watabe, A., Narumiya, S., and Ichikawa, A. (1993) *Biochim. Biophys. Acta* **1175,** 343–350
34. Hasegawa, H., Negishi, M., and Ichikawa, A. (1996) *J. Biol. Chem.* **271,** 1857–1860
35. Hasegawa, H., Katoh, H., Yamaguchi, Y., Nakamura, K., Futakawa, S., and Negishi, M. (2000) *FEBS Lett.* **473,** 76–80
36. Bilson, H. A., Mitchell, D. L., and Ashby, B. (2004) *FEBS Lett.* **572,** 271–275
37. Negishi, M., Hasegawa, H., and Ichikawa, A. (1996) *FEBS Lett.* **386,** 165–168
38. Katoh, H., Aoki, J., Yamaguchi, Y., Kitano, Y., Ichikawa, A., and Negishi, M. (1998) *J. Biol. Chem.* **273,** 28700–28707
39. Riobo, N. A., and Manning, D. R. (2005) *Trends Pharmacol. Sci.* **26,** 146–154
40. Sahai, E., and Marshall, C. J. (2003) *Nat. Cell Biol.* **5,** 711–719
41. Fukui, K., Tamura, S., Wada, A., Kamada, Y., Sawai, Y., Imanaka, K., Kudara, T., Shimomura, I., and Hayashi, N. (2006) *J. Cancer Res. Clin. Oncol.* **132,** 627–633
42. Nelson, P. J., and Daniel, T. O. (2002) *Kidney Int.* **61,** 99–105
43. Yamada, S., and Nelson, W. J. (2007) *J. Cell Biol.* **178,** 517–527